PNAS RESEARCH ARTICLE | MEDICAL SCIENCES

Dermcidin has antiviral activity and protects against influenza

Paula Corell-Escuin[a], Sonia Belmonte-Ballester[b], Anmol Adhav[b], Alberto Marina[b], Laura Gadea-Salom[c], Luis Martinez-Gil[c], Elnaz Aledavood[d], Ana María Fernández-Escamilla[e], Ana Gómez Sáez[f], Nadine Gougeard[b], Kieran Dee[g], Pablo R. Murcia[g], Eliza Adriana Magos[h], Carmen Llena[i], Cristina Peris-Martínez[j,k], Giuseppe D'Auria[l,m], Alejandro Artacho[a], Beatriz Mengual-Chuliá[a,m], F. Xavier López-Labrador[a,m,n], Alex Mira[a,m,1,2], and María Desamparados Ferrer[a,m,1,2]

Affiliations are included on p. 9.

Edited by Laura Martin-Sancho, Imperial College London, London, United Kingdom; received November 25, 2024; accepted February 10, 2026 by Editorial Board Member Adolfo Garcia-Sastre

Despite the high incidence of influenza virus infections, one-fifth of people infected with influenza remain asymptomatic. The mechanisms associated with this immune resilience are, however, unknown. Here, we show that the human antimicrobial peptide dermcidin has antiviral activity against influenza viruses through binding to hemagglutinin and extends its effect to taxonomically unrelated respiratory viruses such as measles virus and human coronavirus OC43. We show that dermcidin is present in all anatomical regions associated with the entry routes of respiratory viruses, that its levels increase during viral respiratory infections, and that it protects mice against influenza disease. Notably, dermcidin levels were higher in asymptomatic individuals than in susceptible peers, suggesting a role in the onset of disease symptoms. Thus, we show that dermcidin inhibits influenza virus infection in vitro and in vivo, with potential as a human-derived product for the prevention and treatment of respiratory viral infections.

dermcidin | respiratory viruses | influenza virus | hemagglutinin | antiviral activity

Significance

This study identifies dermcidin, an antimicrobial peptide previously found in sweat, as a key factor in innate resistance to influenza symptoms. We demonstrate that dermcidin possesses antiviral activity both in vitro and in vivo and establish its link to disease susceptibility. Dermcidin is present in all respiratory virus entry routes (saliva, nasopharynx, and tears), with levels increasing during viral infections. It protects mice from influenza A disease in vivo and exhibits broad-spectrum antiviral activity in vitro, inhibiting all influenza A virus strains tested and other respiratory viruses. These findings underscore dermcidin's potential as an antiviral therapy, offering a promising avenue for combating respiratory viral infections through a naturally occurring human peptide with a unique mechanism of action.

The influenza virus is a leading cause of respiratory infections and a recurrent clinical and public health burden worldwide, with approximately one billion cases diagnosed annually. Of these, 3 to 5 million cases are severe, leading to hospitalization and even death (1). Influenza vaccines are the mainstay of prophylaxis but require annual review due to antigenic drift in the circulating strains (2), and improvements in current treatments are needed. Despite its high prevalence, between 5 and 35% of people exposed to the influenza virus do not develop symptoms (3), but the mechanistic reason for this apparent symptom resistance is not understood (4).

Antimicrobial peptides (AMPs) are small bioactive proteins of up to 50 amino acids in length that are part of the innate immune system and have the potential to be a new source of antimicrobial agents (5). AMPs are generally broad-spectrum, with activity against Gram-positive and -negative bacteria, fungi, and enveloped viruses including HIV (6). Approximately 100 human AMPs have been identified (7) but their small size means that they are generally overlooked in many genetic and proteomic screens (8). Therefore, despite their enormous therapeutic potential, there are no standardized methods for identifying new human AMPs (9).

We hypothesized that resistance to influenza infection symptoms may be due, at least partly, to interindividual variability in the performance of the innate immune system. To test this, we took a functional approach to search for small proteins with potential antiviral activity by generating human cDNA libraries from individuals who have never suffered from influenza-like illness symptoms (hereafter referred to as asymptomatic) with the aim of identifying antiviral peptides (AVPs) that could be responsible for this innate immunity. We found a possible candidate that corresponded to the AMP dermcidin, a protein found in sweat, where it is secreted and processed into several peptides with diverse biological activity (10). We show that dermcidin has antiviral activity against the two main circulating human influenza virus subtypes and other respiratory viruses, including coronavirus and measles virus, and can be found in the main routes of entry of respiratory viruses. We also show that dermcidin levels are higher in asymptomatic individuals, suggesting a protective role in the onset of influenza disease symptoms in humans, and its application in mice reduces viral load in the lungs. These findings reveal the potential of human dermcidin as a natural product for the prevention and treatment of viral respiratory infections.

Results

Screening for AVPs in Individuals Asymptomatic for Influenza Virus Infection. Six human libraries of between 10,000 and 100,000 clones with inserts of ~10 kb were obtained

Author contributions: P.C.-E., A. Mira, and M.D.F. designed research; P.C.-E., S.B.-B., A. Adhav, A. Marina, L.G.-S., L.M.-G., E.A., A.M.F.-E., A.G.S., N.G., and M.D.F. performed research; E.A., A.M.F.-E., K.D., P.R.M., E.A.M., C.L., C.P.-M., F.X.L.-L., and M.D.F. contributed new reagents/analytic tools; P.C.-E., S.B.-B., A. Adhav, G.D.A., A. Artacho, B.M.-C., and M.D.F. analyzed data; and P.C.-E., A. Mira and M.D.F. wrote the paper.

The authors declare no competing interest.

This article is a PNAS Direct Submission. L.M.-S. is a guest editor invited by the Editorial Board.

[1]A. Mira and M.D.F. contributed equally to this work.

[2]To whom correspondence may be addressed. Email: alex.mira@fisabio.es or maria.ferrer@fisabio.es.

This article contains supporting information online at https://www.pnas.org/lookup/suppl/doi:10.1073/pnas.2424461123/-/DCSupplemental.

Published March 30, 2026.

from 19 healthcare workers who, despite continuous direct contact with influenza-infected patients, have never exhibited flu-like symptoms (asymptomatic individuals) (*SI Appendix,* Table S1). Each concentrated pool of proteins (2 to 100 kDa) resulting from the expressed libraries was screened against A/California/7/2009 (H1N1) antigens using standard hemagglutination inhibition (HAI) assay (11). Results showed that one protein mixture derived from the expression of approximately 500 phages inhibited hemagglutination.

As our goal was to search for small molecular weight peptides (a typical AMP molecular weight is ~5 kDa), the positive protein pool was run on an SDS-PAGE gel, and the area of the gel corresponding to 1 to 5 kDa was subjected to peptide mass fingerprinting. Seventy human proteins were identified (*SI Appendix,* Table S2), including dermcidin, the only detected AMP whose antibacterial activity had been previously described (12). Three peptide fragments matching dermcidin and covering 34.6% of its amino acid sequence were identified. Part of the proteolysis-inducing factor (PIF) and propeptide regions were covered by one peptide, and the remaining two peptides aligned with the AMP region (Fig. 1*A*).

Dermcidin Blocks Influenza Virus Infection. The antiviral effect of dermcidin was confirmed by HAI assay with the full-length chemically synthesized peptide corresponding to the AMP region (Fig. 1*A*). This 48 amino acid-long peptide, named DCD-1L (Fig. 1*B*), was tested against the influenza antigens of the A/California/7/2009 (H1N1) strain ("Cal09") in addition to other antigens from the H1N1 and H3N2 subtypes, A/Solomon Islands/03/2006 ("Sol06") and A/Brisbane/10/2007 ("Bris07"), respectively (Fig. 1 *C*, *Left*). DCD-1L was active against the three tested antigens with strain-dependent inhibitor constant (K_i(HAI)) values. We also analyzed the antiviral effect of DCD-1L against infectious influenza viruses. DCD-1L inhibited hemagglutination of both subtypes tested (H1N1 and H3N2) in a subtype-dependent manner (Fig. 1*C*). The K_i(HAI) obtained against the infectious H3N2 subtype strain was up to fourfold higher than that obtained against the H1N1 subtype strain, suggesting that DCD-1L is more active against the H1N1 subtype.

As dermcidin is naturally processed in sweat into different derived peptides (13), we investigated the antiviral activity of nine different naturally processed and truncated dermcidin-derived peptides previously identified in sweat (12, 14) (Fig. 1*B*). No antiviral activity was observed with peptides from the PIF and propeptide regions (YDP-30, YDP-42, and YDP-43) (Fig. 1*C*). Contrastingly, four peptides derived from the AMP region (DCD, SSL-45, LEK-45, and LEK-42) showed antiviral activity in a subtype-dependent manner. Specifically, the peptides with antiviral activity were those with the same net negative charge as DCD-1L (Fig. 1*B*). The only two peptides from the DCD-1L sequence that did not have antiviral activity at the highest concentrations tested (SSL-25 and LEK-24) were those with shorter amino acid lengths (24 and 25 amino acids) and a net positive charge. Also, the only DCD-1L-derived peptide with antiviral activity against all strains of both antigens and infectious influenza virus subtypes was DCD, which differed from DCD-1L only in the elimination of a leucine at the carboxy-terminal end.

With respect to the other three peptides with antiviral activity (SSL-45, LEK-45, and LEK-42), although K_i(HAI) values could not be achieved for antigens of the H3N2 subtype, SSL-45 and LEK-45 (missing three amino acids from the carboxy- and amino-terminus,

A

B

Name	Length (aa)	Sequence	Charge
YDP-30	30	YDPEAASAPGSGNPCHEASAAQKENAGEDP	-4.9
YDP-42	42	YDPEAASAPGSGNPCHEASAAQKENAGEDP GLARQAPKPRKQ-	-0.9
YDP-43	43	YDPEAASAPGSGNPCHEASAAQKENAGEDP GLARQAPKPRKQR	0.1
DCD-1L	48	SSLLEK*GLDGAKKAVGGLGKLGKDAVEDLESVGKGAVHDVKDVLDSVL	-1.8
DCD	47	SSLLEK*GLDGAKKAVGGLGKLGKDAVEDLESVGKGAVHDVKDVLDSV-	-1.8
SSL-45	45	SSLLEK*GLDGAKKAVGGLGKLGKDAVEDLESVGKGAVHDVKDVLD---	-1.8
LEK-45	45	---LEK*GLDGAKKAVGGLGKLGKDAVEDLESVGKGAVHDVKDVLDSVL	-1.8
LEK-42	42	---LEK*GLDGAKKAVGGLGKLGKDAVEDLESVGKGAVHDVKDVLD---	-1.8
SSL-25	25	SSLLEK*GLDGAKKAVGGLGKLGKDA----------	1.9
LEK-24	24	---LEK*GLDGAKKAVGGLGKLGKDAVE----------	0.9

C

Peptide	Viral Antigens		Infectious Viruses	
	H1N1 Sol06	H3N2 Bris07	H1N1 PR8	H3N2 Nor18_H3
YDP-30	>1,000	>1,000	>1,000	>1,000
YDP-42	>1,000	>1,000	>1,000	>1,000
YDP-43	>1,000	>1,000	>1,000	>1,000
DCD-1L	6	10	51*	206
DCD	103	103	103	103
SSL-45	26	>1,000	>1,000	206
LEK-45	51	>1,000	103	411
LEK-42	411	>1,000	>1,000	>1,000
SSL-25	>1,000	>1,000	>1,000	>1,000
LEK-24	>1,000	>1,000	>1,000	>1,000

* Same MIC obtained against A/California/07/2009 antigens

D

Subtype	Strain	IC50 (μM)	95% CI IC50 (μM)	IC90 (μM)
H1N1	PR8	96	79 to 109	223
H1N1	Cal09	254	233 to 276	663
H1N1	Nor18_H1	81	44 to 117	272
H3N2	X-31	133	94 to 172	473
H3N2	Wis09	225	184 to 271	632
H3N2	HK14	167	129 to 206	586
H3N2	Nor18_H3	142	117 to 168	501

Fig. 1. In vitro antiviral activity of dermcidin and its derived peptides against influenza viruses. (*A*) Schematic structure of the unprocessed dermcidin protein (110 aa) composed of a 19 aa signal peptide (Signal) followed by a 30 aa muscle proteolysis-inducing factor (PIF) peptide, a 13 aa propeptide (Propeptide) and a 48 aa C-terminal peptide (AMP) exhibiting antimicrobial activity. The underlined sequence refers to the fragments detected by the peptide mass fingerprint. (*B*) Description, schematic structure, sequences, and charges of the 10 variants derived from dermcidin used in this study, as well as the control peptides DCD-1L^{Ctrl} and DCD1L^{Mut}. Note: K*: acetylated lysine. (*C*) Inhibitor constant values from hemagglutination inhibition assays (*Ki*(HAI)) in μM of ten dermcidin-derived peptides against influenza virus antigens and infectious viruses. "Sol06" denotes A/Solomon Islands/03/06 antigens, "Bris07" denotes A/Brisbane/10/07 antigens, "PR8" denotes A/Puerto Rico/8/34 virus, and "Nor18_H3" denotes A/Norway/3275/18 virus. ">1,000": *Ki*(HAI) not reached within the maximum peptide concentration tested of 1,000 μM. Mean and SEM values are not indicated due to the exact reproducibility of the three independent experiments conducted. (*D*) Half-maximal inhibitory concentration (IC_{50}), 95% CI, and 90% inhibitory concentration (IC_{90}) in μM of the DCD-1L peptide in a plaque inhibition assay on cell lines against influenza virus subtype H1N1 (strains: PR8, "Cal09" denotes A/California/07/09, and "Nor18_H1" denotes A/Norway/3433/18) and against influenza virus subtype H3N2 (strains: "X31" denotes reassortant strain A/Aichi/2/68 (HA,NA) x Puerto Rico/8/34, "Wis09" denotes A/Wisconsin/15/09, Nor18_H3, and "HK14" denotes A/Hong Kong/4801/14).

respectively) were active against the infectious H3N2 strain. With respect to the H1N1 subtype, all three peptides showed activity against the viral antigens tested, with K_i(HAI)s higher than those of the DCD-1L peptide. LEK-45 was the only peptide of this group capable of inhibiting A/Puerto Rico/8/34 ("PR8") infectious virus (Fig. 1 *C*, *Right*). These results suggest that the carboxy-terminal sequence is crucial for the antiviral activity of dermcidin-derived peptides against the H1N1 subtype. Indeed, the LEK-45 peptide was at least 10-fold more active than SSL-45 against PR8.

To further evaluate the antiviral activity of DCD-1L, we performed in vitro inhibition assays in MDCK cells against different strains of H1N1 and H3N2 subtypes. DCD-1L showed antiviral activity against all strains tested, although to varying degrees (Fig. 1*D*). The oldest strains tested, PR8 and X-31, showed half-maximal inhibitory concentration (IC_{50}) values of 96 and 133 μM, respectively, whereas the IC_{50} values against the 2009 strains (Cal09 and Wis09) were 2.6 and 1.7 times higher, respectively. By contrast, the strains dated after the 2009 influenza pandemics (Nor18_H1, Nor18_H3, and HK14) were again more sensitive to DCD-1L treatment, with IC_{50} values similar to those obtained with influenza virus strains before the 2009 pandemic (Fig. 1*D*).

Dermcidin Binds to Viral Hemagglutinin. The antiviral activity of DCD-1L observed in HAI assays suggests that its mechanism of action is mediated by the hemagglutinin (HA) viral envelope protein. To test this hypothesis, affinity assays using microscale thermophoresis (MST) were performed using the DCD-1L peptide with infectious PR8 virus and various PR8-derived virus-like particles (VLPs). The binding affinity results (Fig. 2*A* and *SI Appendix,* Tables S3 and S4) demonstrated that DCD-1L affinity is HA-dependent, with minimal binding observed to VLPs displaying only neuraminidase ("NA") on the surface, in contrast to infectious virus ("PR8"), complete VLPs with HA and NA ("H1, NA"), or VLPs presenting only HA ("H1" and "H3"). These data substantiate that DCD-1L acts by engaging viral HA, thereby blocking the initial step of the influenza virus infection. Furthermore, binding assay results showed that the affinity of DCD-1L for VLPs with only HA from subtype H1N1 (H1) was twice as high as the affinity for VLPs with HAs from subtype H3N2 (H3), consistent with the differential activity observed in both HAI and plaque inhibition assays.

Extending beyond influenza, we investigated the antiviral capacity of DCD-1L against other enveloped respiratory viruses possessing HA-like proteins on their surfaces, including human coronavirus OC43 and measles virus. Results showed that DCD-1L inhibited hemagglutination of both viruses (Fig. 2*B*), supporting an antiattachment mechanism of action, though *Ki*(HAI) values indicated stronger activity against influenza.

To confirm that DCD-1L's antiviral activity depends on its specific amino acid sequence rather than overall net charge, a scrambled control peptide (DCD-$1L^{Ctrl}$) with identical amino acid composition and charge was tested (Fig. 1*B*). DCD-$1L^{Ctrl}$ displayed no inhibition of viral hemagglutination at the concentrations tested (≤206 μM), in contrast to DCD-1L, which exhibited *Ki*(HAI) values of 51 μM for PR8 and OC43, and 26 μM for measles virus. Similarly, no antiviral activity was observed in plaque assays against PR8 at the same concentrations (*SI Appendix,* Table S5). These results robustly demonstrate that DCD-1L's efficacy is governed by its precise sequence and structure conformation, rather than merely its anionic nature.

To gain insight into the potential molecular determinants of DCD-1L's interaction with influenza HA, we performed molecular docking and molecular dynamics (MD) simulations. Three conformations of DCD-1L (open, open-medium, and closed) were considered, and docking analysis versus the HA from PR8 (PDB ID: 6WCR) indicated that all the conformations of DCD-1L were preferentially occupy the conserved stalk region of HA, near the fusion peptide, essential for internalization of the virus into the cell (15) (Fig. 2*C*). The same behavior was observed for the shorter peptides DCD (lacking the leucine at the C-terminal extreme) and LEK-45 (lacking the serine-serine-leucine residues of the N-terminal extreme). In contrast, the other dermcidin-derived peptides with shorter sequences failed to position in the same region, instead, associating closer to the viral membrane, with lower interaction energies and fewer interactions with HA (*SI Appendix,* Fig. S1). These findings may explain their lack of antiviral activity in the HAI assay against strain PR8. MD simulation results showed that DCD-1L remained bound to the stalk region during 270 ns of MD, confirming the stability of the interaction. Analysis of the interfacial region showed that DCD-1L engages predominantly through hydrophobic interactions, complemented by critical hydrogen bonding and salt-bridge interactions with specific stalk residues (Fig. 2*D*). These results underscore the importance of the C-terminal dermcidin contact in stabilizing the binding. In particular, the analysis of the interaction between DCD-1L and HA (*SI Appendix,* Fig. S2) highlighted key DCD-1L residues (S1, E5, K13, V43, L44, or L48) that maintained stable interactions (Fig. 2*D*) for over 80% of the simulation time. Notably, the C-terminal carboxyl group of leucine (L48) formed stabilizing salt-bridge interactions with S290 or K280 in the stalk region. These observations correlate with the HAI assay results, where removal of this residue increased K_i(HAI) values against H1N1 strains, suggesting that DCD-1L engagement with the stalk may allosterically influence the HA globular head. By contrast, MD simulation results of the smallest dermcidin-derived peptide, LEK-24, showed that the peptide left the binding site and diffused into the surrounding solvent after 20 ns, highlighting its instability compared with DCD-1L.

To further validate the DCD-1L binding mode to HA proposed in MD simulations, we evaluated a mutant peptide (DCD-$1L^{Mut}$) bearing two amino acid substitutions, (E5 to L and L44 to E), preserving the amino acid composition and net charge (Fig. 1*B*). This mutant completely lost antiviral activity, with no effect observed at concentrations up to 412 μM in plaque assays, against PR8 and additional H1N1 strain Cal09 (*SI Appendix*, Table S6). These findings reinforce the critical role of these residues proposed by the MD analysis in mediating DCD-1L's interaction with the HA stalk and support a conserved antiviral mechanism across genetically distinct viral backgrounds. We then examined sequence and structural conservation within the predicted DCD-1L binding region of HA. Analysis across over 100 H1 HA variants revealed only minor amino acid differences in the HA2 stalk interaction site (*SI Appendix,* Fig. S3), reflecting the modest strain-specific variations in binding affinity and antiviral potency observed in our cell-based IC_{50} measurements (twofold to threefold variation; Fig. 1*D*). These findings highlight the robust and broadly conserved antiviral activity of DCD-1L, emphasizing that its mechanism of action is maintained across diverse influenza A strains despite minor sequence variation.

Dermcidin Induces Postfusion Conformational Transition of Influenza HA. HAI assays indicated that DCD-1L disrupts sialic acid receptor engagement, implicating interference with HA globular domain mediated recognition. However, molecular docking suggested that the primary interaction site of DCD-1L resides within the stalk domain, raising the question of how this binding event correlates with inhibition of receptor engagement mediated by globular domain. To address this, the ectodomain

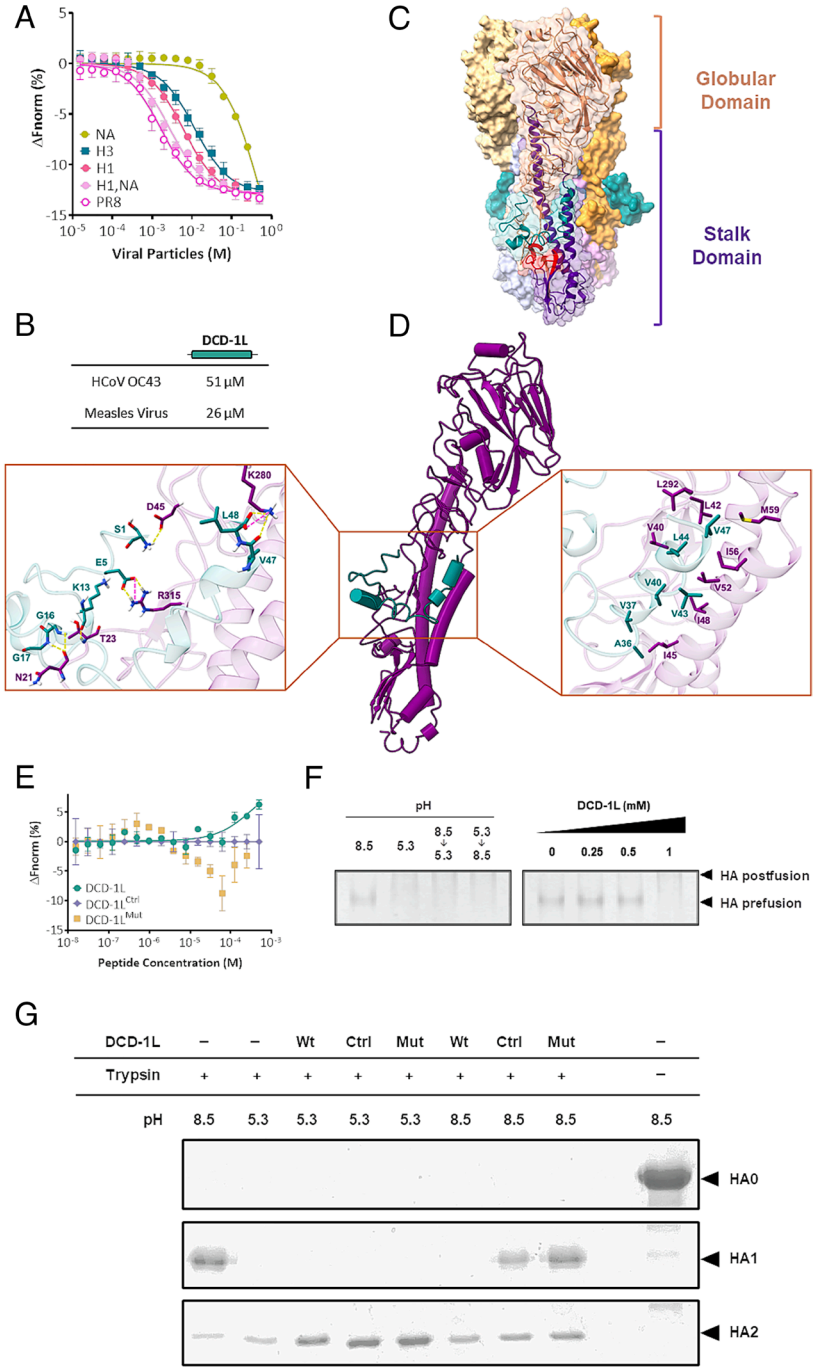

Fig. 2. Dermcidin binds to viral hemagglutinin and induces postfusion conformational transition at neutral pH. (*A*) Dissociation curves measured by microscale thermophoresis of the following: PR8 infectious virus; "H1,NA" noninfectious virus-like particles (VLPs) with hemagglutinin (HA) and neuraminidase (NA) from strain PR8 on the surface; "H1" VLPs with only HA from strain PR8 on the surface; "H3" VLPs with only HA from strain X31 strain on the surface; and "NA" VLPs with only NA from strain PR8 on the surface. Error bars represent the SE of three independent measurements. (*B*) Inhibitor constant *Ki*(HAI) in μM from hemagglutination inhibition assays of DCD-1L against human coronavirus OC43 (HCoV OC43) and measles virus antigens. Mean and SEM values are not indicated due to the exact reproducibility of the three independent experiments conducted. (*C*) Predicted protein–protein interactions between HA of the PR8 strain and the DCD-1L peptide. The functional trimeric HA ectodomain is displayed with its three monomers assembled and represented in cartoon (front monomer) and surface (lateral-back monomers). Globular and stalk domains are colored in different shades of orange and purple, respectively and the fusion peptide is highlighted in red. DCD-1L is rendered in cartoon and colored in teal. (*D*) Key polar interactions (*Left*) and hydrophobic contacts (*Right*) between monomeric HA and DCD-1L peptide after 270 ns of molecular dynamics simulation. The HA monomer is indicated in purple; hydrogen bonds are displayed as yellow dashed lines and salt bridges in pink dashed lines. Residues are numbered according to the numbering in PDB entry 6WCR. (*E*) MST measurements of peptide binding affinities of DCD-1L to HA. Titration curves for DCD-1L (green), DCD-1L^{Ctrl} (purple), and DCD-1L^{Mut} (orange) binding to PR8 HA ectodomain. In the cases of detectable binding, the normalized fluorescence increases with the peptide concentration. The HA-DCD-1L interaction shows binding with a K_D >300 μM but the precise value could not be determined, as aggregation effects were observed at peptide concentrations exceeding 1 mM. Error bars indicate the SE from three independent measurements. (*F*) Native-PAGE of HA under different pH conditions (*Left*) and DCD-1L concentrations (*Right*) shows that DCD-1L binding at neutral pH promotes a similar conformational change that the observed in the prefusion to postfusion transition induced by acidic pH. (*G*) Trypsin susceptibility assay in the presence of DCD-1L, DCD-1L^{Mut}, or DCD-1L^{Ctrl}. Exposition to acidic pH (5.3) induces postfusion conformation that renders HA2 stalk domain sensitive to trypsin digestion meanwhile this domain is trypsin-resistant in the prefusion conformation at neutral pH (7.4). Incubation with DCD-1L at neutral pH promotes HA2 trypsin susceptibility characteristic of postfusion conformation. By contrast, DCD-1L^{Mut} and DCD-1L^{Ctrl} do not promote HA from trypsin digestion at this pH.

of PR8 HA was recombinantly produced, and its interaction with DCD-1L was assessed using MST. DCD-1L, but not DCD-1L^{Ctrl} or DCD-1L^{Mut} peptides, exhibited binding to HA (Fig. 2*E*). Consistent with our *in* vivo experiments, MST assays revealed low affinity between HA for DCD-1L (Kd > 300 μM). However, accurate determination of the dissociation constant was precluded by aggregation at higher peptide concentrations. Native-PAGE analysis attributed the observed aggregation to HA rather than the peptide, suggesting that DCD-1L binding may induce a conformational change in HA that promotes aggregation (Fig. 2*F*). The most prominent conformational transition of HA during viral entry is the shift from the prefusion to the postfusion state, typically triggered by low pH within the endosome to facilitate virus–host membrane fusion. Strikingly, native-PAGE analysis confirms that DCD-1L induces at neutral pH, which resembles the postfusion state observed under acidic conditions (Fig. 2*F*), supporting the hypothesis that DCD-1L promotes the postfusion conformation of HA independently of pH. To further validate this conformational shift, protease susceptibility assays were performed. This assay, widely recognized as a marker of the HA postfusion state, relies on the increased protease sensitivity of the HA2 stalk subunit following low pH-induced conformational rearrangement, whereas this domain at the prefusion conformation remains protease (16). The assay showed that DCD-1L renders HA susceptible to proteases at neutral pH, whereas neither DCD-1L^{Ctrl} nor DCD-1L^{Mut} promote the conformational change that induces such susceptibility (Fig. 2*G*). Taken together, these findings demonstrate that DCD-1L induces a conformational transition in HA from the prefusion to the postfusion state at neutral pH. This report describes an influenza virus inhibitor that exerts its antiviral

effect by promoting the postfusion conformation of HA at neutral pH. This mechanism explains how DCD-1L binding to the stalk region of HA interferes with viral recognition and engagement, thereby blocking entry into target host cells.

Dermcidin Is Produced in Anatomical Sites of Respiratory Virus Entry. Given the antiviral activity of dermcidin, we explored its production in the main routes of entry of respiratory viruses into the human body, the mouth, nose, and eyes. Results showed that dermcidin is produced naturally in the three main routes of respiratory virus entry, albeit at lower concentrations than those observed in sweat (17). The average concentrations obtained ranged between 15.5 ng/mL in nasopharyngeal samples, 35 ng/mL in saliva, and 180 ng/mL in tears (*SI Appendix,* Fig. S4*A*). Furthermore, the concentration in saliva samples remained constant throughout the day, suggesting that dermcidin production does not follow a circadian rhythm (*SI Appendix,* Fig. S4*B*). Because dermcidin is secreted in sweat by the eccrine glands (17), we investigate the origin of its production inside the oral cavity (*SI Appendix,* Fig. S4*C*), finding that the major contribution to salivary dermcidin was made by the parotid gland (*SI Appendix,* Fig. S4*D*).

Dermcidin Is Elevated in Asymptomatic Individuals, and Not Associated with Genetic Sequence Variations. The dermcidin gene (*DCD*) was analyzed in individuals classified as asymptomatic or susceptible to influenza-like illness symptoms. The genetic structure of *DCD* and the percentage of individuals with each of the mutations found in both groups are shown in Fig. 3 *A* and *B*, respectively, and detailed information is summarized in *SI Appendix,* Table S7. Although several synonymous and nonsynonymous mutations were found in the exons of some individuals, these differences could not be significantly associated with specific peptide variants in either group of individuals.

We also compared the basal nasopharyngeal and saliva-dermcidin concentrations in both susceptible and asymptomatic individuals. Basal levels of dermcidin in healthy subjects were higher in asymptomatic individuals than in susceptible peers (Fig. 3 *C* and *D*), being significant in nasopharyngeal samples ($P < 0.0001$) where the peptide concentration was about sixfold higher (Fig. 3*C*). These results suggest that the higher basal levels of dermcidin in the nasopharynx of asymptomatic individuals, rather than the presence of a given peptide variant, might be contributing to their innate resistance to influenza virus symptoms.

Dermcidin Is Overproduced in Respiratory Viral Infections. Because the production of human AMPs can be induced by microbial infections (18), we investigated whether dermcidin levels increased during influenza virus infection. Salivary dermcidin levels in 16 patients admitted during influenza virus infection (positive for influenza virus RNA by real-time RT-PCR) were analyzed and compared with the basal levels in the same individuals 4 mo after infection. The results showed that mean salivary levels of dermcidin were significantly higher during influenza infection (Fig. 4*A*).

Given the antiviral potential of dermcidin against other respiratory viruses, we investigated whether dermcidin production is elevated in response to other viral infections. To this end, nasopharyngeal (Fig. 4*B*) and salivary (Fig. 4*C*) dermcidin levels were measured in hospitalized individuals positive for other respiratory viruses (real-time RT-PCR positive for RNA from respiratory syncytial virus, metapneumovirus, parainfluenza, rhinovirus, adenovirus, bocavirus, or coronavirus), as well as inpatients positive for influenza virus by real-time RT-PCR, and were compared with basal levels of dermcidin of individuals susceptible to influenza-like illness symptoms at healthy state ("Susceptible"). Results showed that patients infected with respiratory viruses had significantly higher levels of dermcidin than healthy individuals, especially in nasopharyngeal samples.

DCD-1L Is Nontoxic and Tolerable in Mice. Although dermcidin is naturally produced in the human body, we evaluated cytotoxicity in vitro and safety in vivo. Cytotoxicity assays in MDCK cells were performed with dermcidin and its derived peptides showing antiviral activity. Although a decrease in cell viability was observed, this was not dose-dependent and was maintained at all concentrations, not exceeding 20% at the highest concentration tested (*SI Appendix,* Fig. S5).

To evaluate the tolerability of DCD-1L, BALB/c mice were treated intranasally with 50 mg/kg/d of DCD-1L in a single-dose regimen and in a 4-dose regimen (corresponding to 20 times the IC_{50} against strain PR8). Neither dosage regimen induced significant changes in body weight, clinical signs (*SI Appendix,* Fig. S6), or histopathological features. Therefore, a 4-d dosing regimen of 1 mg per day of DCD-1L peptide was safe in vivo.

We also investigated the body distribution of DCD-1L after intranasal administration. A signal peak in the nostrils, lung, liver, and digestive tract was observed between 3 and 6 h after treatment with the peptide labeled with a fluorophore (*SI Appendix,* Fig. S7), with a lower signal observed in various organs up to 24 h. Fluorescence results revealed that DCD-1L was metabolized and excreted by the urinary tract.

DCD-1L Protects Mice against Influenza Virus Disease. Finally, we performed an experimental infection challenge to assess the anti-influenza efficacy of DCD-1L in mice. Four experimental study groups were compared: a zanamivir (positive control) group, a placebo (negative control) group, and two DCD-1L groups (one group received DCD-1L 3 h after infection [postinfection] and the other group received a mixture of DCD-1L coincubated with the virus for 1 h before administration [coincubated]; see Fig. 5*A* for details). Daily measurements of body weight revealed weight loss up to 10% in the placebo and DCD-1L postinfection groups at day 6 postinfection, a threshold commonly used in murine influenza studies to indicate moderate disease severity (19) (Fig. 5*B*). Furthermore, half of the mice in both groups began to show clinical signs of disease from day 6 after infection. Contrastingly, the survival rate and clinical score in the coincubated and zanamivir groups were unaffected throughout the study (Fig. 5*C*).

No difference was observed in lung viral load between postinfection and placebo groups (Fig. 5*D*). By contrast, viral replication was significantly suppressed in the coincubated group at day 6 postinfection, similar to zanamivir group. In addition, although viral load remained consistently low until day 10 postinfection in the coincubated group, there were no significant differences compared with the placebo group at the end of the study. Overall, these findings show that DCD-1L can protect against influenza virus disease when coincubated with the virus prior to infection and maintains a low viral load up to 10 d after infection.

Discussion

Influenza viruses cause varying degrees of respiratory illness, from asymptomatic cases to acute respiratory syndrome, and are responsible for high rates of morbidity and mortality worldwide (3, 20). The incidence of asymptomatic influenza infection fluctuates from 9.4 to 90% of cases, depending on viral strain, season, and the criteria used to identify asymptomatic cases (3, 21); nevertheless, the mechanisms behind this immune resilience remain unclear (

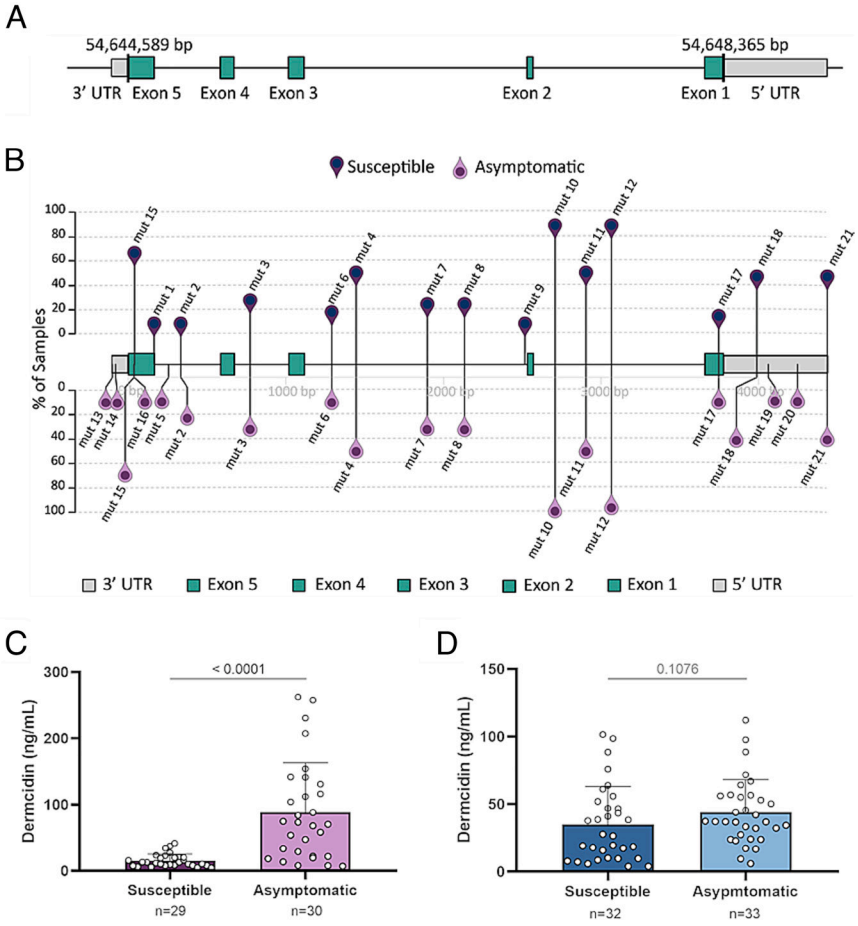

Fig. 3. Asymptomatic individuals have elevated dermcidin levels and do not carry unique dermcidin genetic variants. (*A*) Human *DCD* gene structure on chromosome 12q13.2. (*B*) Lollipop plot illustrating *DCD* mutations, distributed into the percentage of individuals (Samples) of the cohort of 31 susceptible and 36 asymptomatic individuals to influenza infection. Dermcidin levels of (*C*) nasopharyngeal and (*D*) saliva samples from healthy individuals who have experienced influenza symptoms in the past (Susceptible) and those who have never experienced influenza-like illness symptoms (Asymptomatic). Points represent individual samples and bars represent mean ± SD. The number of individuals per group is shown below. A nonparametric Mann–Whitney test was applied and the corresponding p-values are indicated in each graph.

4, 22). The term "asymptomatic" generally implies prior exposure to the virus; however, despite healthcare workers from hospital intensive care units—such as those involved in this study—being at a significantly higher risk of influenza exposure (23), our study did not empirically validate this assumption. Therefore, although a more precise term might have been preferable for accurately describing individuals who have never experienced flu symptoms and have not been vaccinated, we deliberately chose this term to ensure the clear communication of our intended meaning. Our findings suggest that the innate resistance to influenza-like illness may be associated with increased production of dermcidin. Other studies have shown that reduced production of dermcidin is associated with noninfectious diseases such as cancers (24–29), and immunosuppressive diseases such as psoriasis (30), and atopic dermatitis (17), among others (31).

Antibacterial and antifungal activities associated with dermcidin have also been well described (12). However, our results support its antiviral activity and its potential role in determining susceptibility or resistance to a respiratory viral disease. Dermcidin appears to act as a first, nonspecific line of immune defense, providing protection against colonization and infection (6). It is the most abundant AMP in sweat (32), and has been detected not only in skin tissues (12), but also in a broad range of secretions such as basal tears (33), sinonasal secretions (34), and breast milk (35). Notably, we demonstrate that dermcidin is produced in the main entry routes for respiratory viruses, such as nasopharynx, tears, and saliva, highlighting a crucial role in the first line of defense against infections.

Asymptomatic individuals had higher dermcidin levels than those susceptible to common flu symptoms, suggesting that the inherently higher dermcidin levels in nasopharynx may confer protection against respiratory viral infections. Given that influenza viruses primarily target airway epithelial cells, the elevated dermcidin in the nasal could enhance immune defenses, lowering the risk of respiratory viral infections. Interestingly, the difference in dermcidin levels between susceptible and asymptomatic individuals could not be linked to genetic variations in *DCD*. Further studies are therefore needed to investigate the regulatory features that control the overproduction of the dermcidin peptide in asymptomatic individuals, such as epigenetic modifications or variations in gene copy number in relevant tissues.

Dermcidin is abundantly present in mucosal secretions, although the concentrations required for antiviral activity in vitro (80 to 250 μM) exceed typical physiological levels measured in vivo (~0.02 μM in nasal secretions). Nevertheless, multiple lines of evidence support a functional role for dermcidin in mucosal immunity. Mucosal surfaces such as the oral cavity and nasopharynx are continuously bathed in large volumes of fluid—saliva alone ranges from 0.5 to 1.5 L per day (36)—with secretion volume increasing in response to infection (37). This abundant and dynamically replenished fluid milieu can sustain local dermcidin concentration and availability, while glandular output, particularly from the parotid, ensures continuous replenishment. In addition to its local concentration, dermcidin likely acts synergistically with other innate immune factors in mucosal secretions, a mechanism well-documented for host defense peptides, enhancing antiviral activity beyond what is observed in isolated in vitro conditions (38). Importantly, increasing evidence suggests that dermcidin also exerts immunomodulatory effects. While this function has not been extensively studied in the respiratory tract, dermcidin has been reported to induce cytokine production, including TNF-α, IL-8, CXCL10, and CCL20 in keratinocytes (39), and to modulate TNF-α production in LPS-stimulated monocytes (40), suggesting

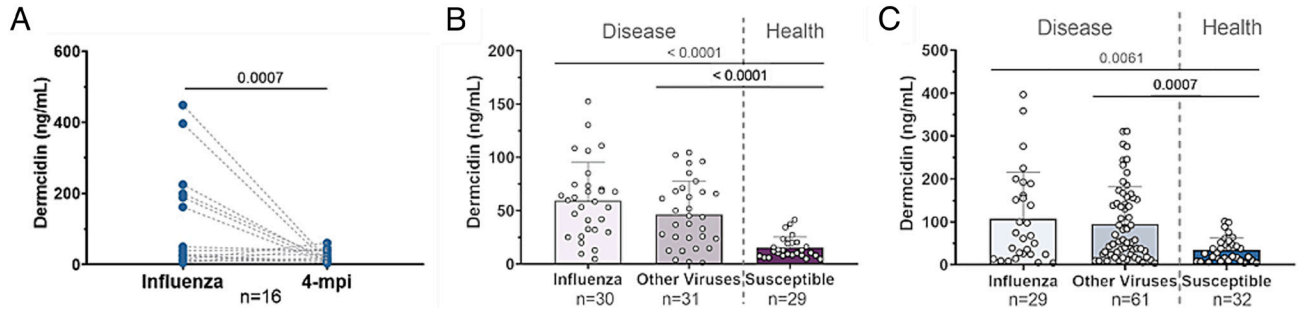

Fig. 4. Overproduction of dermcidin in response to respiratory viral infections. Dermcidin levels of (*A*) saliva samples from symptomatic individuals to influenza virus during infection (Influenza) and 4 mo postinfection (4-mpi) (n = 16). Blue dots represent paired samples and dotted-gray lines link each individual. Wilcoxon test was applied, and the *P*-value is indicated in the graph. Dermcidin levels of (*B*) nasopharyngeal and (*C*) saliva samples from hospitalized individuals positive for influenza virus RNA by real-time RT-PCR (Influenza), hospitalized individuals positive by real-time RT-PCR for RNA from other respiratory viruses (Other Viruses), and healthy individuals who have experienced influenza symptoms in the past (Susceptible). Points represent individual samples and bars represent mean ± SD. The number of individuals per group is shown below each column. A paired Mann–Whitney test was applied between groups and the corresponding *P*-values are indicated.

a broader role beyond direct viral inhibition. This dual functionality is consistent with its expression pattern, which resembles other multifunctional host defense peptides such us β-defensin 2 and the cathelicidin LL-37, both of which orchestrate immune cell responses while promoting viral clearance through direct and indirect mechanisms (38, 41, 42). Therefore, while in vitro IC_{50} values provide a useful benchmark, they do not fully capture the complex physiological and immunological environment in which dermcidin operates at mucosal surfaces. Taken together, these observations highlight not only the direct antiviral potential of dermcidin, but also its likely contribution to mucosal immunity via immunomodulatory pathways, underscoring the need for further investigation into its multifaceted role in host defense.

We found that the in vivo levels of dermcidin increase in response to respiratory virus infections, which is consistent with what is observed for other human defensins such as the human cathelicidin LL-37 (43). Some studies have also shown that LL-37 has antiviral activity against influenza virus, adenovirus, respiratory syncytial virus, and HIV (44–46), but showed reduced efficacy against the pandemic strain H1N1pdm09 (47). Notably, we found that dermcidin is active against all strains and subtypes of influenza A virus tested. Our findings revealed a possible link between the antiviral potential of dermcidin and its net charge, which is −1.8, unlike most human defensins, which are typically cationic. Importantly, this activity is not merely a consequence of dermcidin's unusual net negative charge. A scrambled control peptide and a second peptide mutant in two positions, both with identical composition and charge than DCD-1L showed no antiviral activity, in contrast to native DCD-1L, which displayed robust antiviral effects. These results underscore that dermcidin's efficacy arises from its precise amino acid sequence and structural conformation, rather than from charge alone.

Our initial HAI assays indicated that DCD-1L interferes with receptor engagement mediated by the globular domain. Nevertheless, computational modeling indicated that the peptide predominantly associates with the highly conserved stalk domain, providing a plausible explanation for its broad-spectrum antiviral activity against both Group 1 (e.g., H1N1) and Group 2 (e.g., H3N2) influenza A viruses (48). Sequence analysis of multiple HA variants revealed only minor sequence differences within the predicted DCD-1L interaction region of the HA stalk, which is consistent with our cell-based IC_{50} measurements showing modest strain-specific variations across influenza A isolates (*SI Appendix*, Fig. S3). These observations further underscore the broadly conserved antiviral activity of DCD-1L across influenza variants.

To interrogate and corroborate this mechanistic model, we performed in vitro biochemical assays using recombinantly produced HA ectodomain, which demonstrated that DCD-1L binding triggers an irreversible transition of HA toward the postfusion conformation, effectively incapacitating the globular domain receptor-binding site. In support of this proposed mechanism, the two DCD-1L variants, the scrambled and mutant, that retains the same net charge and amino acid composition, failed to induce the HA postfusion conformational transition, thereby subtly corroborating the mechanistic model of stalk interaction underlying DCD-1L function. To date, several compounds, small proteins and antibodies have been described that block the HA transition between the prefusion and postfusion states of HA (49–52), which has been proposed as therapeutical tools for inhibition of influenza virus fusion. However, the mechanism of action observed for DCD-1L is novel. As far as we know, only one compound has previously been reported to promote this conformational change, and in that case, the action of the compound is restricted to potentiates the natural low-pH-induced conversion of HA (51). In contrast, DCD-1L induces the postfusion conformation of HA at neutral pH. While these results provide strong functional evidence, future structural studies to visualize DCD-1L binding will be required to fully elucidate this mechanism of action.

The mechanism of action of commercial WHO-approved antivirals such As oseltamivir and zanamivir relies on neuraminidase inhibition, thereby preventing progeny virion release (53). However, their clinical use is largely restricted to severely ill or immunosuppressed patients due to the rapid emergence of resistant strains (54). In contrast, dermcidin engages the highly conserved stalk region, a strategy expected to limit resistance and confer broad-spectrum activity across influenza A subtypes and other HA-bearing respiratory viruses. By irreversibly driving HA into the postfusion state, dermcidin effectively blocks viral engagement and entry at its earliest stage, exploiting an intrinsic vulnerability of the fusion machinery and thereby establishing a mechanism fundamentally distinct from currently approved neuraminidase inhibitors. Beyond this direct antiviral mechanism, the conformational rearrangement induced by dermcidin may also unmask cryptic epitopes on HA normally hidden in the prefusion state, potentially enhancing immune recognition and facilitating broader antiviral responses (55). Moreover, dermcidin has been reported to display immunomodulatory activities in other epithelial contexts, raising the possibility that its antiviral effects are complemented by host-directed activities at mucosal surfaces. Taken together, these findings support a model in which dermcidin not

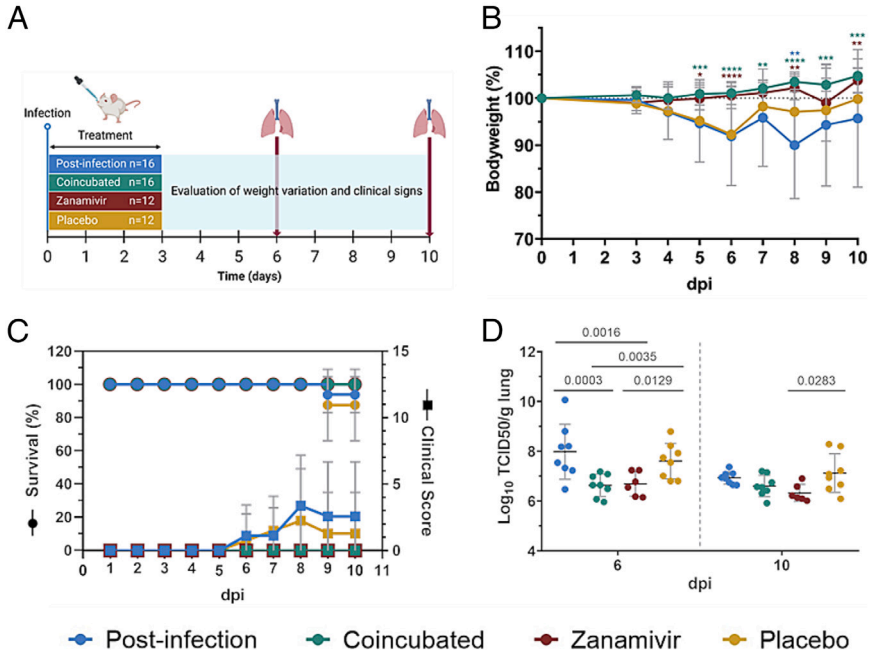

Fig. 5. DCD-1L peptide protects against influenza virus disease in mice. (*A*) Experimental study groups and timeline of the protocol. Mice were intranasally infected with 10^2 plaque-forming units of influenza virus strain PR8. The "Postinfection" group was treated with 50 mg/kg/d of DCD-1L peptide 3 h after infection and one daily dose for the following 3 d. The "Coincubated" group was infected with a mixture of virus plus DCD-1L, previously coincubated for 1 h at room temperature; the treatment of 1 mg/mouse/d was continued for the following 3 d. The "Zanamivir" group was treated with 40 μg/mouse/d of the antiviral 3 h after infection; the treatment was followed with the same dose for the following 3 d. The "Placebo" group was mock-treated with 25 μL of PBS following the same dosing regimen as the antiviral control. Body weight and the presence of clinical signs were registered daily. Lung samples were obtained on days 6 and 10 after infection. (*B*) Percentage of body weight variation relative to initial weight, expressed as mean ± SEM. Dunnett's multiple comparisons test was applied against Placebo and the *P*-values are indicated in the graphs as * < 0.05, ** < 0.01, and **** < 0.0001. (*C*) Disease kinetics as percentage of survival (*Left Y* axis) and average clinical score (*Right Y* axis). Clinical scores were assigned on a scale of 0 to 3 for each of the following clinical signs: ruffled fur, hunched posture, labored breathing, and dehydration. Values are represented as mean ± SEM. Dunnett's multiple comparisons test was applied, and no significant *P*-values were obtained. (*D*) Viral titers in the homogenized lungs of mice at 6 and 10 d postinfection. Data are presented as $\log_{10}$ $TCID_{50}$ values per gram of tissue of the individual mice (points). Black horizontal lines represent mean values and gray error bars indicate SD. A Mann–Whitney test was applied and the corresponding *P*-values are indicated.

only neutralizes influenza virus through premature induction of the postfusion state of HA, but also could contribute to host defense by enhancing viral immunogenicity and engaging additional immune pathways. While future structural and immunological studies will be required to define the extent and significance of these complementary activities, the observed in vivo efficacy of dermcidin highlights its translational potential as an antiviral strategy.

In vivo protection was evaluated in a murine model using a sublethal PR8 challenge, a commonly used model in influenza research (56). Under these conditions, dermcidin was effective in reducing viral load (~1 $\log_{10}$) when coincubated with the virus prior to infection, with an efficacy similar to zanamivir. This reduction, both biologically and statistically significant, is in line with decreases observed for other antiviral agents, including oseltamivir (56). Nevertheless, the protective effect was lost when DCD-1L was administered 3 h after infection. This behavior has also been observed with other AMPs, such as human neutrophil peptides, where direct incubation of peptides and viruses was required (57). In the case of these other AMPs, the lack of antiviral effects when administered postinfection appears to be related to their mechanism of action, which induces viral aggregation (44). In contrast, as dermcidin binds to viral HA, its lack of antiviral activity in the posttreatment group could be due to an insufficient amount to block viral uptake effectively or the rapid metabolism of the peptide after application. This was supported by the low levels of DCD-1L detected in mice 24 h after administration. Increasing the amount administered and/or designing a delivery system for prolonged drug release may be a plausible solution.

AMPs can prevent microbial colonization, have low drug resistance, act as immunomodulators, and have minimal side effects, together with their potential for scale-up in industrial production, making them excellent candidates for therapeutic and prophylactic agents (58). In addition, the broad spectrum of antimicrobial activity associated with dermcidin would be highly beneficial in treating influenza disease, as this infection is usually accompanied by a secondary bacterial infection (59). In conclusion, the present study provides valuable insights into the potential of dermcidin as a biomarker of severe susceptibility to influenza infection and also as an antiviral agent to combat influenza virus infections, offering hope for the development of an antiviral treatment based on a naturally produced human peptide.

Materials and Methods

For additional information, please see *SI Appendix, SI Materials and Methods*.

Antiviral peptides were identified from phage display libraries constructed with mouthwash samples from asymptomatic healthcare workers and screened by hemagglutination inhibition, with active fractions resolved by LC–MS/MS. Chemically synthesized dermcidin-derived peptides, including scrambled and mutant controls, were tested against influenza A strains in MDCK and MDCK-SIAT1 cells using hemagglutination inhibition and plaque reduction assays, while cytotoxicity was evaluated by cell viability assays. Peptide–HA interactions were characterized by microscale thermophoresis. Protein–protein docking and molecular dynamics simulations were performed to model the peptide–HA binding interface, and sequence conservation of the DCD-1L binding site on PR8 HA was assessed. Recombinant PR8 HA ectodomain was produced in a baculovirus–insect cell system and used for biochemical assays, including native PAGE and trypsin susceptibility. In vivo biodistribution, tolerability, and efficacy were

assessed following intranasal peptide administration in BALB/c mice, while dermcidin levels and genetic variants were analyzed in human samples by ELISA and sequencing. Statistical analyses were performed using nonparametric tests or generalized linear models as appropriate; details are provided in the *SI Appendix*.

Data, Materials, and Software Availability. Genetic sequences repository data have been deposited in European Nucleotide Archive (ENA) under the project PRJEB75383 https://www.ebi.ac.uk/ena/browser/view/PRJEB75383 (60). Other data are included in the article and/or *SI Appendix*.

ACKNOWLEDGMENTS. This study was supported by grants INNVAL20/19/006 and INNVA2/2021/3 from the Valencian Innovation Agency (AVI), FISABIO Innovation grant PAPIRO UGP-21-047, an EXPLORA Action from the Spanish Ministry of Science and Innovation with code SAF2013-505553-EXP, CIPROM/2023/30 from Regional Ministry of Education, Culture, Universities, and Employment of the Valencian Government, PID2022-137201NB-I00 from the Spanish Ministry of Science and Innovation and by the Carlos III Health Institute, under file code CP22/00036, pursuant to the Resolution of the Director of the Carlos III Health Institute, O.A., M.P., dated December 7, 2022, granting the Miguel Servet Contracts, and cofinanced by the European Union. We thank the patients and the IBSP-CV Biobank (PT17/0015/0017) integrated in the Spanish National Biobanks Network and in the Valencian Biobanking Network for collaboration. We also thank the Central Service for Experimental Research of Universitat de València for the sequencing. Finally, we express our gratitude to Dr. Elena Tapia, Eduardo Romanos, Dr. Julián Pardo, and Dr. Maykel Arias from Instituto Aragonés de Ciencias de la Salud for assistance with the animal experiments, to Dr. Florian Krammer for kindly providing baculoviruses expressing PR8 HA ectodomain, Dr. Jeronimo Bravo for sharing insect High Five cells and to Kenneth McCreath for helpful comments on the manuscript. E.A. and A.M.F.-E. thank Dr. Carmen Gil and Dr. Ana Martínez for valuable advice and for providing access to computational resources. Some of the figure graphics were created by using BioRender.com.

Author affiliations: [a]Genomics and Health Unit, Fundació per al Foment de la Investigació Sanitària i Biomèdica de la Comunitat Valenciana - Salut Pública, Valencia 46020, Spain; [b]Macromolecular Crystallography Unit, Institute of Biomedicine of Valencia, Spanish National Research Council and Biomedical Research Networking Center for Rare Diseases, Instituto de Salud Carlos III, Valencia 46010, Spain; [c]Department of Biochemistry and Molecular Biology, Universitat de València, Burjassot, Valencia 46100, Spain; [d]Group of Translational Medicinal and Biological Chemistry, Margarita Salas Centre for Biological Research, Spanish National Research Council, Madrid 28040, Spain; [e]Antiviral Strategies Unit, Instituto de Investigación, Desarrollo e Innovación en Biotecnología, Elche, Alicante 03202, Spain; [f]Department of Molecular Cell Biology and Immunology, Amsterdam University Medical Center, Amsterdam 1007 MB, The Netherlands; [g]Medical Research Council-University of Glasgow Centre for Virus Research, Institute of Infection, Immunity and Inflammation, College of Medical, Veterinary and Life Science, University of Glasgow, Glasgow G61 1QH, United Kingdom; [h]Department of Health of Castellón, Castellón Provincial Hospital Consortium, Castellón de la Plana, Castellón 12002, Spain; [i]Department of Stomatology, Faculty of Medicine and Dentistry, Universitat de València, Valencia 46010, Spain; [j]Unit of Cornea and Anterior Eye Diseases, Fundación de Oftalmología Medica, Valencia 46015, Spain; [k]Department of Surgery (Ophthalmology), Faculty of Medicine, Universitat de València, Valencia 46010, Spain; [l]Sequencing and Bioinformatics Service, Fundació per al Foment de la Investigació Sanitària i Biomèdica de la Comunitat Valenciana - Salut Pública, València 46020, Spain; [m]Biomedical Research Networking Center for Epidemiology and Public Health, Instituto de Salud Carlos III, Madrid 28029, Spain; and [n]Department of Microbiology and Ecology, University of Valencia Medical School, Valencia 46010, Spain

1. M. P. Girard, T. Cherian, Y. Pervikov, M. P. Kieny, A review of vaccine research and development: Human acute respiratory infections. *Vaccine* **23**, 5708–5724 (2005).
2. A. S. Monto, J. G. Petrie, Improving influenza vaccine effectiveness: Ways to begin solving the problem. *Clin. Infect. Dis.* **69**, 1824–1826 (2019).
3. L. Furuya-Kanamori *et al.*, Heterogeneous and dynamic prevalence of asymptomatic influenza virus infections. *Emerg. Infect. Dis.* **22**, 1052–1056 (2016).
4. J. L. Casanova, L. Abel, The human genetic determinism of life-threatening infectious diseases: Genetic heterogeneity and physiological homogeneity? *Hum. Genet.* **139**, 681–694 (2020).
5. F. Asif, S. U. Zaman, M. K. H. Arnab, M. Hasan, M. M. Islam, Antimicrobial peptides as therapeutics: Confronting delivery challenges to optimize efficacy. *The Microbe* **2**, 100051 (2024).
6. J. Talapko *et al.*, Antimicrobial peptides–Mechanisms of action, antimicrobial effects and clinical applications. *Antibiotics* **11**, 1417 (2022).
7. G. Wang, Human antimicrobial peptides and proteins. *Pharmaceuticals* **7**, 545–594 (2014).
8. K. A. Silverstein *et al.*, Small cysteine-rich peptides resembling antimicrobial peptides have been under-predicted in plants. *Plant J.* **51**, 262–280 (2007).
9. W. F. Porto, A. S. Pires, O. L. Franco, Computational tools for exploring sequence databases as a resource for antimicrobial peptides. *Biotechnol. Adv.* **35**, 337–349 (2017).
10. M. Paulmann *et al.*, Structure-activity analysis of the dermcidin-derived peptide DCD-1L, an anionic antimicrobial peptide present in human sweat. *J. Biol. Chem.* **287**, 8434–8443 (2012).
11. World Health Organization, *Manual for the Laboratory Diagnosis and Virological Surveillance of Influenza* (World Health Organization, 2011).
12. B. Schittek *et al.*, Dermcidin: A novel human antibiotic peptide secreted by sweat glands. *Nat. Immunol.* **2**, 1133–1137 (2001).
13. B. Schittek, The multiple facets of dermcidin in cell survival and host defense. *J. Innate Immun.* **4**, 349–360 (2012).
14. S. Rieg *et al.*, Expression of the sweat-derived innate defence antimicrobial peptide dermcidin is not impaired in *Staphylococcus aureus* colonization or recurrent skin infections. *Clin. Exp. Dermatol.* **39**, 209–212 (2014).
15. S. C. Harrison, Viral membrane fusion. *Virol. J.* **479**, 498–507 (2015).
16. J. J. Skehel *et al.*, Changes in the conformation of influenza virus hemagglutinin at the pH optimum of virus-mediated membrane fusion. *Proc. Natl. Acad. Sci. U.S.A.* **79**, 968–972 (1982).
17. S. Rieg *et al.*, Deficiency of dermcidin-derived antimicrobial peptides in sweat of patients with atopic dermatitis correlates with an impaired innate defense of human skin *in vivo*. *J. Immunol.* **174**, 8003–8010 (2005).
18. X. Xia, L. Cheng, S. Zhang, L. Wang, J. Hu, The role of natural antimicrobial peptides during infection and chronic inflammation. *Antonie Van Leeuwenhoek.* **111**, 5–26 (2018).
19. N. M. Bouvier, A. C. Lowen, Animal models for influenza virus pathogenesis and transmission. *Viruses* **2**, 1530–1565 (2010).
20. A. D. Iuliano *et al.*, Estimates of global seasonal influenza-associated respiratory mortality: A modelling study. *Lancet* **391**, 1285–1300 (2018).
21. N. H. Leung, C. Xu, D. K. Ip, B. J. Cowling, The fraction of influenza virus infections that are asymptomatic: A systematic review and meta-analysis. *J. Epidemiol.* **26**, 862–872 (2015).
22. S. K. Ahuja *et al.*; South Texas Veterans Health Care System COVID-19 team, Immune resilience despite inflammatory stress promotes longevity and favorable health outcomes including resistance to infection. *Nat. Commun.* **14**, 3286 (2023).
23. S. P. Kuster *et al.*, Incidence of influenza in healthy adults and healthcare workers: A systematic review and meta-analysis. *PLoS One* **6**, e26239 (2011).
24. D. A. C. Deans *et al.*, Expression of the proteolysis-inducing factor core peptide mRNA is upregulated in both tumour and adjacent normal tissue in gastro-oesophageal malignancy. *Br. J. Cancer.* **94**, 731–736 (2006).
25. Y. Minami *et al.*, Immunohistochemical staining of cutaneous tumours with G-81, a monoclonal antibody to dermcidin. *Br. J. Dermatol.* **151**, 165–169 (2004).
26. G. D. Stewart, R. J. Skipworth, J. A. Ross, K. C. Fearon, V. E. Baracos, The dermcidin gene in cancer: Role in cachexia, carcinogenesis and tumour cell survival. *Curr. Opin. Clin. Nutr. Metab. Care.* **11**, 208–213 (2008).
27. F. Qiu *et al.*, Dermcidin enhances the migration, invasion, and metastasis of hepatocellular carcinoma cells in vitro and in vivo. *J. Clin. Transl. Hepatol.* **10**, 429–438 (2022).
28. W. C. Chang *et al.*, Dermcidin identification from exhaled air for lung cancer diagnosis. *Eur. Respir. J.* **35**, 1182–1185 (2010).
29. L. Núñez-Naveira, L. A. Mariñas-Pardo, C. Montero-Martínez, Mass spectrometry analysis of the exhaled breath condensate and proposal of dermcidin and S100A9 as possible markers for lung cancer prognosis. *Lung* **197**, 523–531 (2019).
30. D. Che *et al.*, Dermcidin-derived polypeptides: DCD (86–103) induced inflammatory reaction in the skin by activation of mast cells via ST2. *Immunol. Lett.* **251**, 29–37 (2022).
31. R. Ghosh, U. K. Maji, R. Bhattacharya, A. K. Sinha, The role of dermcidin isoform 2: A two-faceted atherosclerotic risk factor for coronary artery disease and the effect of acetyl salicylic acid on it. *Thromb. J.* **2012**, 987932 (2012).
32. É. Csősz, G. Emri, G. Kalló, G. Tsaprailis, J. Tőzsér, Highly abundant defense proteins in human sweat as revealed by targeted proteomics and label-free quantification mass spectrometry. *J. Eur. Acad. Dermatol. Venereol.* **29**, 2024–2031 (2015).
33. J. You *et al.*, Post-translation modification of proteins in tears. *Electrophor.* **31**, 1853–1861 (2010).
34. E. E. Cottrill *et al.*, Expression of dermcidin in human sinonasal secretions. *Int. Forum Allergy Rhinol.* **7**, 154–159 (2017).
35. B. D. Chow *et al.*, Host defense proteins in breast milk and neonatal yeast colonization. *J. Hum. Lact.* **32**, 168–173 (2016).
36. S. P. Humphrey, R. T. Williamson, A review of saliva: Normal composition, flow, and function. *J. Prosthet. Dent.* **85**, 162–169 (2001).
37. Y. Igarashi *et al.*, Analysis of nasal secretions during experimental rhinovirus upper respiratory infections. *J. Allergy Clin. Immunol.* **92**, 722–731 (1993).
38. R. E. Hancock, E. F. Haney, E. E. Gill, The immunology of host defence peptides: Beyond antimicrobial activity. *Nat. Rev. Immunol.* **16**, 321–334 (2016).
39. F. Niyonsaba *et al.*, The human antimicrobial peptide dermcidin activates normal human keratinocytes. *Br. J. Dermatol.* **160**, 243–249 (2009).
40. E. Wang, X. Qiang, J. Li, S. Zhu, P. Wang, The *in vitro* immune-modulating properties of a sweat gland-derived antimicrobial peptide dermcidin. *Shock* **45**, 28–32 (2016).
41. D. Yang, O. Chertov, J. J. Oppenheim, Participation of mammalian defensins and cathelicidins in anti-microbial immunity: Receptors and activities of human defensins and cathelicidin (LL-37). *J. Leukoc. Biol.* **69**, 691–697 (2001).
42. M. Zanetti, Cathelicidins, multifunctional peptides of the innate immunity. *J. Leukoc. Biol.* **75**, 39–48 (2004).
43. S. M. Currie *et al.*, Cathelicidins have direct antiviral activity against respiratory syncytial virus *in vitro* and protective function *in vivo* in mice and humans. *J. Immunol.* **196**, 2699–2710 (2016).
44. I. N. Hsieh, K. L. Hartshorn, The role of antimicrobial peptides in influenza virus infection and their potential as antiviral and immunomodulatory therapy. *J. Pharm.* **9**, 53 (2016).
45. D. Vandamme, B. Landuyt, W. Luyten, L. Schoofs, A comprehensive summary of LL-37, the factotum human cathelicidin peptide. *Cell. Immunol.* **280**, 22–35 (2012).
46. P. G. Barlow *et al.*, Antiviral activity and increased host defense against influenza infection elicited by the human cathelicidin LL-37. *PLoS One* **6**, e25333 (2011).
47. S. Tripathi *et al.*, Antiviral activity of the human cathelicidin, LL-37, and derived peptides on seasonal and pandemic influenza A viruses. *PLoS One* **10**, e0124706 (2015).
48. M. Agamennone *et al.*, Antiviral peptides as anti-influenza agents. *Int. J. Mol. Sci.* **23**, 11433 (2022).

49. M. J. van Dongen *et al.*, An orally active small molecule fusion inhibitor of influenza virus. *Science* **363**, eaar6221 (2019).
50. Y. Chen *et al.*, Structural basis for a human broadly neutralizing influenza A hemagglutinin stem-specific antibody including H17/18 subtypes. *Nat. Commun.* **13**, 7603 (2022).
51. L. R. Hoffman, I. D. Kuntz, J. M. White, Structure-based identification of an inducer of the low-pH conformational change in the influenza virus hemagglutinin: Irreversible inhibition of infectivity. *J. Virol.* **71**, 8808–8820 (1997).
52. S. J. Fleishman *et al.*, Computational design of proteins targeting the conserved stem region of influenza hemagglutinin. *Science* **332**, 816–821 (2011).
53. R. J. Jackson *et al.*, Oseltamivir, zanamivir and amantadine in the prevention of influenza: A systematic review. *J. Infect.* **62**, 14–25 (2011).
54. V. Correia, L. A. Santos, M. Géria, M. M. Almeida-Santos, H. Rebelo-de-Andrade, Influenza A (H1N1) pdm09 resistance and cross-decreased susceptibility to oseltamivir and zanamivir antiviral drugs. *J. Med. Virol.* **87**, 45–56 (2015).
55. K. Tonouchi *et al.*, Structural basis for cross-group recognition of an influenza virus hemagglutinin antibody that targets postfusion stabilized epitope. *PLoS Pathog.* **19**, e1011554 (2023).
56. R. W. Sidwell, D. F. Smee, In vitro and in vivo assay systems for study of influenza virus inhibitors. *Antivir. Res.* **48**, 1–16 (2000).
57. K. L. Hartshorn, M. R. White, T. Tecle, U. Holmskov, E. C. Crouch, Innate defense against influenza A virus: Activity of human neutrophil defensins and interactions of defensins with surfactant protein D. *J. Immun.* **176**, 6962–6972 (2006).
58. D. K. Govindarajan, K. Kandaswamy, Antimicrobial peptides: A small molecule for sustainable healthcare applications. *Med. Microecol.* **18**, 100090 (2023).
59. K. Liderot, M. Ahl, V. Özenci, Secondary bacterial infections in patients with seasonal influenza A and pandemic H1N1. *BioMed Res. Int.* **2013**, 376219 (2013).
60. P. Corell-Escuin, Sequence data from "Project PRJEB75383." European Nucleotide Archive. https://www.ebi.ac.uk/ena/browser/view/PRJEB75383. Deposited 4 November 2024.